

# Single-Mode 1.3- $\mu\text{m}$ Photonic Crystal Vertical-Cavity Surface-Emitting Laser

Paul O. Leisher, *Student Member, IEEE*, Aaron J. Danner, *Member, IEEE*, and Kent D. Choquette, *Fellow, IEEE*

**Abstract**—We report the use of a photonic crystal in a 1.3- $\mu\text{m}$  vertical-cavity surface-emitting laser to achieve single fundamental-mode operation. A focused ion beam was used to mill the photonic crystal into a top dielectric distributed Bragg reflector. The laser operated continuous-wave at room temperature with greater than 1 mW of single-mode output power observed with a sidemode suppression ratio of more than 37 dB and little change to the electrical properties of the device.

**Index Terms**—Photonic crystal, vertical-cavity surface-emitting laser (VCSEL).

## I. INTRODUCTION

VERTICAL-CAVITY surface-emitting lasers (VCSELs) are attractive sources for optical data communication for a variety of reasons including their suitability for low-cost, high volume manufacture, compatibility for on-wafer testing, and the ability to easily fabricate arrays. However, VCSELs have historically suffered from poor performance at the standard telecommunication wavelengths of 1.3 and 1.55  $\mu\text{m}$  due to the challenges of epitaxial growth of suitable gain materials with effective distributed Bragg reflectors (DBRs). The desire to use VCSELs as sources for communication over longer distances has motivated research in a variety of long-wavelength VCSEL technologies [1]–[4].

Single fundamental-mode operation of VCSEL sources is crucial to high-speed optical data communication applications with low dispersion. However, because the transverse dimensions are much larger than the effective cavity length in the longitudinal direction, standard VCSEL designs typically lead to operation in multiple transverse modes. A variety of methods have been explored for achieving fundamental-mode operation of 850-nm VCSELs [5]–[11].

In this work, photonic crystal patterns are designed and fabricated in 1.3- $\mu\text{m}$  VCSELs containing InGaAsN quantum wells and hybrid DBR designs. The resulting device characteristics are compared to unetched control devices to determine the effectiveness of the photonic crystal to produce single transverse mode operation.

## II. EXPERIMENT

Previously fabricated 1.3- $\mu\text{m}$  VCSELs containing InGaAsN quantum wells were used in this experiment [3], [4]. The struc-

Manuscript received June 12, 2006; revised July 10, 2006. This work was supported by the National Science Foundation under Grant 03-35082, and by the Center for Microanalysis of Materials, which is partially supported by the U.S. Department of Energy Grant DEFG02-91-ER45439.

The authors are with the Micro and Nanotechnology Laboratory, Department of Electrical and Computer Engineering, University of Illinois at Urbana-Champaign, Urbana, IL 61801 USA (e-mail: pleisher@ieec.org; adanner@vcSEL.micro.uiuc.edu; choquette@uiuc.edu).

Digital Object Identifier 10.1109/LPT.2006.883189

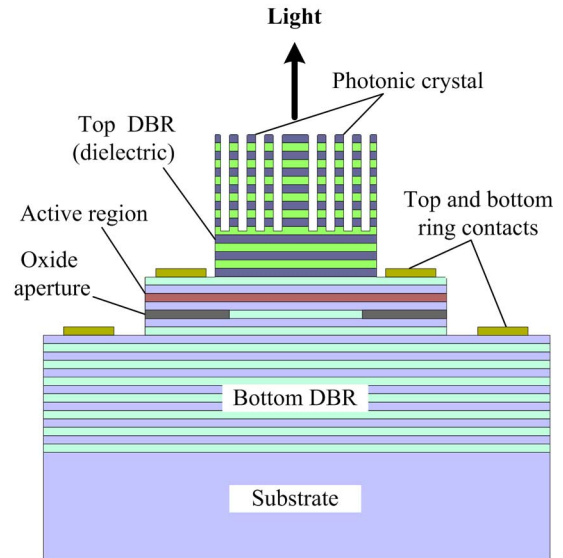


Fig. 1. Cross-sectional schematic for the photonic crystal VCSEL. (Color version available online at <http://ieeexplore.ieee.org>.)

ture, as illustrated in Fig. 1, consists of a bottom AlGaAs-based DBR grown on a GaAs substrate with a highly strained InGaAsN quantum-well-based active region. Current confinement is provided by an 8- $\mu\text{m}$  diameter oxide aperture, and ohmic ring contacts are formed on both sides of the active region. The top DBR is formed by alternating dielectric layers, and the VCSELs are designed to operate at approximately 1.3  $\mu\text{m}$ .

Following the procedure originally outlined by Yokouchi *et al.* in [8], a single defect photonic crystal is designed for single-mode operation for this VCSEL structure. An out-of-plane photonic band diagram is computed using the plane-wave expansion method for a photonic crystal with a hole diameter ( $b$ ) to lattice constant ( $a$ ) ratio,  $b/a = 0.5$ . Using this band diagram, the effective index of the photonic crystal region  $n_{\text{PhC}}$  is computed under the assumption that the holes are etched infinitely deep. Because the photonic crystal is not etched completely through the structure, it is necessary to correct the computed refractive index for the finite etch depth. We use an etch depth dependence factor of  $\gamma = 0.1$  to 0.3, which corresponds to an etch approximately 60% to 80% the way through the top DBR [8]. The  $V$ -parameter can be calculated and used to evaluate the expected modal properties of the device by

$$V_{\text{eff}} = \frac{\pi D}{\lambda_o} \sqrt{n_1^2 - n_2^2}. \quad (1)$$

The wavelength of operation is  $\lambda_o$ , and the waveguide diameter  $D$  is a function of the photonic crystal and defect. For a single

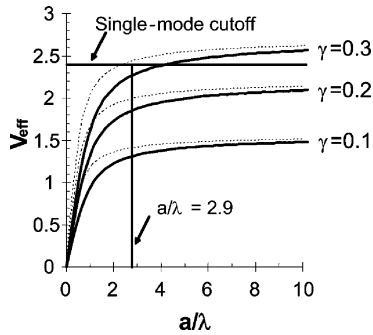


Fig. 2. Calculated  $V_{\text{eff}}$  as a function of the photonic crystal normalized frequency ( $a/\lambda$ ). The three pairs of curves correspond to three etch depths. The calculation is performed for bulk  $\text{SiO}_2$  (solid) and bulk  $\text{SiN}_x$  (dashed), with the VCSEL solution lying between the two. The laser reported herein operates at  $a/\lambda = 2.9$ .

defect photonic crystal,  $D = 2a - b$ . The “core” index  $n_1$  is given by the index of the unetched DBR in the defect, the “clad” index is  $n_2 = \gamma n_{\text{PhC}} + (1 - \gamma)n_1$ , and  $n_{\text{PhC}}$  is the index of refraction which is calculated from the band diagram. If  $V_{\text{eff}}$  is less than 2.4 and the corresponding index contrast is sufficient to dominate over thermal instabilities ( $n_1 - n_2 > 10^{-3}$ ), the device is expected to operate in the single fundamental mode [8], [9].

In general, this method assumes a negligible difference in the index of refraction of the layers in the DBR (the index of refraction for all layers in the DBR is approximately given by  $n_1$ ). This is not the case in our current structure because of the larger index contrast between each mirror layer of the dielectric DBR stack. Therefore, we calculate  $V_{\text{eff}}$  for both bulk  $\text{SiO}_2$  and bulk  $\text{SiN}_x$ , with the solution for our VCSEL lying somewhere between the two constituent layers of the mirror. Fig. 2 illustrates the calculated  $V_{\text{eff}}$  as a function of the normalized frequency for the photonic crystal. This shows the designed single-defect photonic crystal VCSEL with  $b/a = 0.5$  should operate single-mode, provided  $\gamma < 0.3$ .

The photonic crystal patterns were directly incorporated into the top DBR using focused ion beam (FIB) milling [12]. Each pattern was milled at an ion beam current of 3000 pA for approximately 4 min 15 s, resulting in an etch depth of approximately 2  $\mu\text{m}$ . The etch rate was calibrated by performing similar FIB milling and step profilometry analysis. This depth was chosen such that the resulting index contrast was large enough to dominate over thermal instabilities, but not so deep as to encroach on the semiconductor-dielectric interface or push  $V_{\text{eff}}$  beyond the single-mode cutoff condition. Fig. 3 depicts an optical microscope image of a completed photonic crystal VCSEL.

The fabricated 1.3- $\mu\text{m}$  photonic crystal VCSELs were characterized using on-wafer probing at room temperature. Continuous-wave light versus current ( $L-I$ ) characteristics were measured using a semiconductor parameter analyzer to vary the input current and measure the output of a germanium photodetector, and the output spectrum at maximum power was measured using an optical spectrum analyzer.

### III. RESULTS

The output spectrum at maximum power for an unpatterned, but otherwise identical, control device is shown in Fig. 4(a). At

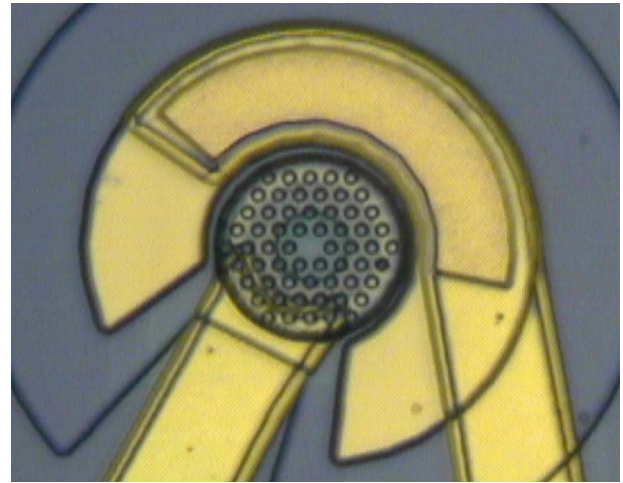


Fig. 3. Optical microscope image of a photonic crystal VCSEL. The hole diameter to lattice constant ratio  $b/a$  is 0.5 and the lattice spacing  $a$  is 3.7  $\mu\text{m}$ . (Color version available online at <http://ieeexplore.ieee.org>.)

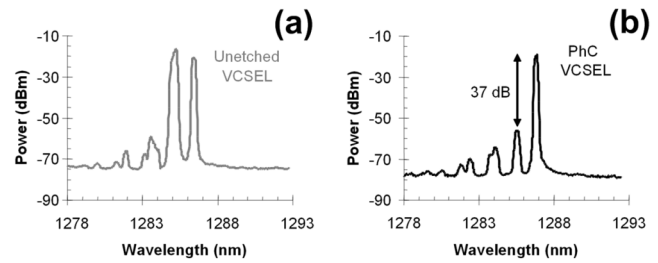


Fig. 4. Optical lasing spectrum taken at rollover for an (a) unetched control and (b) etched photonic crystal VCSEL with dielectric DBR operating at  $\sim 1.3 \mu\text{m}$ .

this injection level, the control device is clearly operating multimode, with two transverse modes at 1285 and 1286 nm. Multimode operation was confirmed at a variety of injection current levels from threshold to rollover. Fig. 4(b) illustrates the output spectrum at maximum power for the photonic crystal VCSEL. Stable single-mode operation, defined as  $>30$ -dB side-mode suppression ratio (SMSR), was achieved over the entire operating range of the VCSEL, as illustrated in Fig. 5(a). This particular device had photonic crystal parameters  $b/a = 0.5$  and  $a = 3.7 \mu\text{m}$ . The estimated hole etch depth of 2  $\mu\text{m}$  corresponds to  $\gamma \approx 0.2$ . From Fig. 2, we clearly see a large tolerance in the actual depth of the holes for predictable single-mode operation, and determine a nominal  $V_{\text{eff}} \approx 1.9$ , with corresponding index contrast  $\Delta n \approx 3 \times 10^{-3}$ . These values are consistent with the observed stable single-mode operation of the VCSEL.

Fig. 5(b) shows the  $L-I$  characteristics for both the unpatterned control and photonic crystal VCSEL. The photonic crystal VCSEL exhibits lower, albeit single-mode output power. Increased scattering loss due to the presence of the etched holes leads to an increase in threshold current. This increased loss combined with an approximate 50% reduction in modal volume produces the decrease in total output power. However, greater than 1 mW of single-mode output power was still observed for the photonic crystal VCSEL. Additionally, the rollover current was slightly decreased due to the increase of threshold current and a reduction in device heat dissipation which was introduced by the etched holes. The current-voltage ( $I-V$ ) characteristics

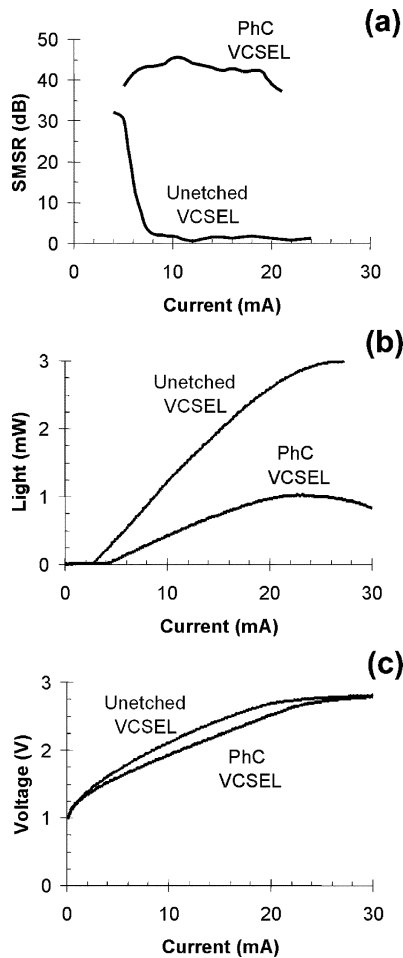


Fig. 5. (a) SMSR versus injected current, (b) output power versus injected current, and (c) voltage versus injected current for the unetched control and etched  $1.3\text{-}\mu\text{m}$  photonic crystal VCSELs.

for both the unpatterned control and photonic crystal VCSEL are shown in Fig. 5(c). Because the photonic crystal is milled into a dielectric DBR, the  $I$ - $V$  characteristics for both devices are not significantly different.

This photonic crystal VCSEL differs from prior work in two important ways. First, we have shown that by incorporating the milled pattern into a dielectric (as opposed to semiconductor) DBR, the transverse optical mode can be designed independent of the electrical properties of the VCSEL. Second, we show the design methodology originally proposed for single-mode  $850\text{-nm}$  photonic crystal VCSELs can be extended to long wavelength VCSELs.

#### IV. CONCLUSION

We have demonstrated single fundamental-mode operation of a  $1.3\text{-}\mu\text{m}$  photonic crystal VCSEL. An FIB was used to mill the photonic crystal into the top dielectric DBR. Greater than  $1\text{ mW}$  of single-mode output power was observed with an SMSR of

more than  $37\text{ dB}$  without much change to the electrical properties of the device. Because of the relatively large dimensions of the photonic crystal, particularly at this longer wavelength, this method of reliably designing and reproducing single-mode operation could be achieved using standard photolithography followed by reactive ion etching, making this method well-suited to low-cost high-volume manufacture. Single-mode VCSELs based on etched photonic crystal patterns may improve long wavelength optical communication applications due to their increased fiber coupling efficiency, reduced chromatic dispersion, and compatibility with existing telecommunication systems.

#### ACKNOWLEDGMENT

The authors would like to thank D. Kisker and Optical Communications Products, Inc.

#### REFERENCES

- [1] H. Soda, K. Iga, C. Kitahara, and Y. Suematsu, "GaInAsP/inp surface emitting injection lasers," *Jpn. J. Appl. Phys.*, vol. 18, no. 12, pp. 2329–2330, 1979.
- [2] J. J. Dudley, D. I. Babić, R. Mirin, L. Yang, B. I. Miller, R. J. Ram, T. Reynolds, E. L. Hu, and J. E. Bowers, "Low threshold wafer fused long wavelength vertical cavity lasers," *Appl. Phys. Lett.*, vol. 64, no. 12, pp. 1463–1465, 1994.
- [3] K. D. Choquette, J. F. Klem, A. J. Fischer, O. Blum, A. A. Allerman, I. J. Fritz, S. R. Kurtz, W. G. Breiland, R. Sieg, K. M. Geib, J. W. Scott, and R. L. Naone, "Room temperature continuous wave InGaAsN quantum well vertical-cavity lasers emitting at  $1.3\text{ }\mu\text{m}$ ," *Electron. Lett.*, vol. 36, no. 16, pp. 1388–1390, 2000.
- [4] A. W. Jackson, R. L. Naone, M. J. Dalberth, J. M. Smith, K. J. Malone, D. W. Kisker, J. F. Klem, K. D. Choquette, D. K. Serkland, and K. M. Geib, "OC-48 capable InGaAsN vertical cavity lasers," *Electron. Lett.*, vol. 37, no. 6, pp. 355–356, 2001.
- [5] C. Jung, R. Jäger, M. Grabherr, P. Schnitzer, R. Michalzik, B. Weigl, S. Müller, and K. J. Ebeling, "4.8 mW singlemode oxide confined top-surface emitting vertical-cavity laser diodes," *Electron. Lett.*, vol. 33, no. 21, pp. 1790–1791, 1997.
- [6] H. Martinsson, J. A. Vukusic, M. Grabherr, R. Michalzik, R. Jäger, K. J. Ebeling, and A. Larsson, "Transverse mode selection in large-area oxide-confined vertical-cavity surface-emitting lasers using a shallow surface relief," *IEEE Photon. Technol. Lett.*, vol. 11, no. 12, pp. 1536–1538, Dec. 1999.
- [7] D. S. Song, S. H. Kim, H. G. Park, C. K. Kim, and Y. H. Lee, "Single-fundamental-mode photonic-crystal vertical-cavity surface-emitting lasers," *Appl. Phys. Lett.*, vol. 80, no. 21, pp. 3901–3903, 2002.
- [8] N. Yokouchi, A. J. Danner, and K. D. Choquette, "Etching depth dependence of the effective refractive index in two-dimensional photonic-crystal-patterned vertical-cavity surface-emitting laser structures," *Appl. Phys. Lett.*, vol. 82, no. 9, pp. 1344–1346, 2003.
- [9] A. J. Danner, J. J. Raftery Jr., P. O. Leisher, and K. D. Choquette, "Single mode photonic crystal vertical cavity lasers," *Appl. Phys. Lett.*, vol. 88, p. 091114, 2006.
- [10] A. Furukawa, S. Sasaki, M. Hoshi, A. Matsuzono, K. Moritoh, and T. Baba, "High-power single-mode vertical-cavity surface-emitting lasers with triangular holey structure," *Appl. Phys. Lett.*, vol. 85, no. 22, pp. 5161–5163, 2004.
- [11] P. O. Leisher, A. J. Danner, J. J. Raftery Jr., and K. D. Choquette, "Proton implanted single mode holey vertical-cavity surface emitting lasers," *Electron. Lett.*, vol. 41, no. 18, pp. 1010–1011, 2005.
- [12] Y. K. Kim, A. J. Danner, J. J. Raftery Jr., and K. D. Choquette, "Focused ion beam nanopatterning for optoelectronic device fabrication," *IEEE J. Sel. Topics Quantum Electron.*, vol. 11, no. 6, pp. 1292–1298, Nov./Dec. 2005.